

UCLA

UCLA Previously Published Works

Title

Next-generation liquefaction database

Permalink

<https://escholarship.org/uc/item/0v6770q3>

Journal

Earthquake Spectra, 36(2)

ISSN

8755-2930

Authors

Brandenberg, Scott J
Zimmaro, Paolo
Stewart, Jonathan P
[et al.](#)

Publication Date

2020-05-01

DOI

10.1177/8755293020902477

Peer reviewed

1 Next Generation Liquefaction Database

2 **Scott J. Brandenberg,^{a)} M.EERI, Paolo Zimmaro,^{b)} M.EERI, Jonathan P.**
3 **Stewart,^{c)} M.EERI, Dong Youp Kwak,^{d)} M.EERI, Kevin W. Franke,^{e)} M.EERI,**
4 **Robb E.S. Moss,^{f)} M.EERI, K. Önder Çetin,^{g)} Gizem Can,^{h)} Makbule Ilgac,ⁱ⁾**
5 **John Stamatakos,^{j)} M.EERI, Thomas Weaver,^{k)} and Steven L. Kramer,^{l)}**
6 **M.EERI,**

7 The Next Generation Liquefaction database is a resource for the geotechnical
8 hazard community. It is publicly available online under the following digital object
9 identifier (DOI): 10.21222/C2J040. The database organizes objective liquefaction
10 data into tables and fields (columns of information), with the relationships among
11 the tables and fields described by a schema. The data is organized into tables
12 pertaining to (i) sites, including geotechnical and geophysical site investigation
13 data, surface geology information, and laboratory test data, (ii) earthquake events,
14 including source and ground motion information, and (iii) observations of sites
15 following events. The schema was vetted through community outreach efforts
16 involving multiple workshops and meetings. Users can view the data, download
17 existing data, and upload new data through a geographic information system (GIS)-
18 based graphical user interface. Information uploaded to the database is reviewed by
19 a database working group to verify consistency between uploaded data and source
20 documents. The database is replicated in DesignSafe where users can interact with

^{a)} Department of Civil and Environmental Engineering, 5731 Boelter Hall, University of California, Los Angeles, CA 90095

^{b)} Department of Civil and Environmental Engineering, 5731 Boelter Hall, University of California, Los Angeles, CA 90095

^{c)} Department of Civil and Environmental Engineering, 5731 Boelter Hall, University of California, Los Angeles, CA 90095

^{d)} Department of Civil and Environmental Engineering, Hanyang University, 55 Hanyangdaehak-ro, Sangnok-gu, 111 Engineering Building II, Ansan, Gyeonggi-do, 15588, Republic of Korea

^{e)} Department of Civil and Environmental Engineering, Brigham Young University, 368 Clyde Bldg., Provo, UT, 84602

^{f)} Department of Civil and Environmental Engineering, Cal Poly, San Luis Obispo, CA 93407

^{g)} Department of Civil Engineering, Middle East Technical University, 06800 Çankaya, Ankara, Turkey

^{h)} Department of Civil Engineering, Middle East Technical University, 06800 Çankaya, Ankara, Turkey

ⁱ⁾ Department of Civil Engineering, Middle East Technical University, 06800 Çankaya, Ankara, Turkey

^{j)} Southwest Research Institute, 1801 Rockville Pike, Rockville, MD, 20852-1633

^{k)} U.S. Nuclear Regulatory Commission, Office of Research, Washington, DC 20555-0001

^{l)} Department of Civil Engineering, More Hall Rm. 132E, Box 352700, Seattle, WA 98195-2700

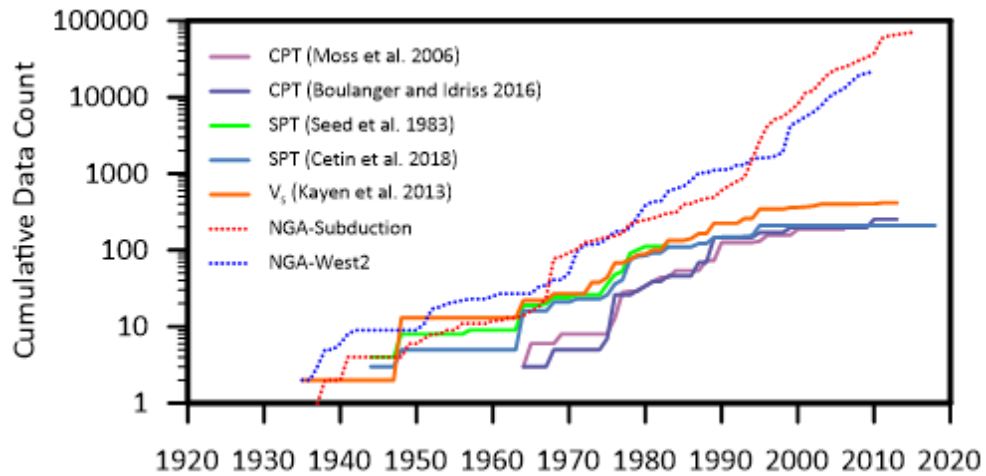
21 the data using Python scripts in Jupyter notebooks, view point cloud data using
22 Potree, and interact with geospatial data using QGIS.

23 INTRODUCTION

24 Semi-empirical procedures for evaluating liquefaction susceptibility, triggering, and effects
25 combine empirical observations with various aspects of theory. Measurements of penetration
26 resistance [e.g., Seed et al. (1983), Çetin et al. (2004) and (2018), Idriss and Boulanger (2012),
27 for standard penetration test, SPT; Robertson and Wride (1998), Moss et al. (2006), Boulanger
28 and Idriss (2016) for cone penetration test, CPT], or shear wave velocity, V_s [e.g., Andrus and
29 Stokoe (2000), Kayen et al. (2013)] are generally utilized to assess soil resistance to
30 liquefaction. Qualitative geology-based criteria can also be used to estimate relative levels of
31 liquefaction resistance (Youd and Hoose, 1977; Youd and Perkins, 1978; Obermeier et al.,
32 1990; Lewis et al., 1999). In a similar manner, liquefaction resistance at the regional scale can
33 be modeled using geospatial variables (Zhu et al., 2015 and 2017). Surface ground motion
34 parameters are combined with wave propagation theory to estimate stress demands at a
35 particular depth, and this demand is compared with resistance to obtain a factor of safety or the
36 probability of liquefaction given a certain event. For this reason, procedures for evaluating
37 liquefaction rely strongly on empirical data. An analogous data-driven model development
38 approach has been adopted by the various Next Generation Attenuation (NGA) projects (e.g.
39 NGA-West2, Bozorgnia et al. 2014 for shallow crustal earthquakes in active tectonic regions;
40 NGA-East, Goulet et al. 2018 for stable continental regions; and NGA-Subduction, Kishida et
41 al. 2017, for subduction events). A goal of the NGL project is to facilitate a similar process for
42 modeling liquefaction triggering and consequences.

43 Variations over time of the cumulative numbers of case histories in the SPT, CPT, and V_s
44 liquefaction databases are presented in Figure 1 along with the cumulative numbers of ground
45 motion records in the NGA-West2 and NGA-Subduction projects. The number of ground
46 motion records in the NGA projects has grown exponentially with time, as indicated by the
47 essentially linear slope in semi-log space in Figure 1. The liquefaction databases, by contrast,
48 show essentially exponential growth from about 1960 to 1995, but the growth has slowed
49 recently, with very few new case histories introduced into these databases since 1995. This
50 trend is not due to a lack of available data. For example, the Canterbury Earthquake Sequence
51 in 2010 and 2011 produced tens of thousands of cone penetration tests with observations of
52 ground performance during multiple earthquakes (e.g., van Ballegooy et al. 2014; Maurer et

53 al. 2014). Furthermore, post-1995 earthquakes that have produced potential liquefaction case
 54 history information include: 1999 Kocaeli, 1999 Chi-Chi, 1999 Duzce, 2001 Bhuj, 2001
 55 Nisqually, 2001 Peru, 2002 Denali, 2004 Niigata Chuetsu-Oki, 2007 Niigata Ken Chuetsu-
 56 Oki, 2007 Pisco, 2008 Iwate, 2009 L'Aquila, 2010 Maule, 2010 El Mayor Cucapah, 2011
 57 Tohoku-Oki, 2012 Emilia, 2015 Nepal, 2016 Kaikoura, 2017 Puebla, 2018 Hokkaido Eastern
 58 Iburi, 2018 Anchorage, and 2019 Ridgecrest.



59
 60 **Figure 1.** Cumulative number of liquefaction case histories utilized in various triggering models, and
 61 ground motion records in the NGA-West2 and NGA-Subduction projects.

62
 63 We believe that liquefaction case history databases have lagged behind the exponential
 64 growth exhibited by the ground motion databases because the NGA projects involved a broad
 65 community effort surrounding database development, whereas development of liquefaction
 66 datasets has largely been undertaken by small research groups [i.e., Seed et al. (1983) and Çetin
 67 et al. (2004 and 2018) for standard penetration test (SPT) data, Moss et al. (2006) for cone
 68 penetration test (CPT) data, Kayen et al. (2013) for shear-wave velocity (V_s) data, and Zhu et
 69 al., (2015) for geospatial data] without a broader organizational framework. A larger
 70 community effort is needed to optimize the potential to learn from recent events and grow the
 71 liquefaction database both in size and quality. The need for a publicly available liquefaction
 72 database was the first recommendation of the committee commissioned by the National
 73 Academies of Sciences, Engineering, and Medicine to address the state of the art and practice
 74 in assessment of earthquake-induced liquefaction and its consequences (National Academies
 75 2016):

76 "Recommendation 1. Establish curated, publicly accessible databases of relevant
77 liquefaction triggering and consequence case history data. Include case histories in
78 which soils interact with built structures. Document the case histories with relevant
79 field, laboratory, and physical model data. Develop the databases with strict
80 protocols and include indicators of data quality."

81 The Next-Generation Liquefaction (NGL) project was designed in part to address this clear
82 need. NGL is a multi-year community-based effort consisting of three components: (1) a
83 transparent, open-source liquefaction database, (2) supporting studies for effects that should be
84 captured in models but that cannot be constrained by case history data, and (3) model
85 development (Stewart et al. 2016).

86 This paper presents the structure of the NGL relational database, and the graphical user
87 interface (GUI) developed to upload, view, and download data. We also discuss the review
88 process implemented to ensure that uploaded data are consistent with source documents. The
89 GUI allows users to interact with the data in a limited manner, but model developers will need
90 to work with the data in ways that are not implemented in the GUI. For this reason, the database
91 is periodically replicated in DesignSafe, a cyberinfrastructure for the natural hazards
92 community (Rathje et al. 2017). This allows users to formulate their own queries, perform high
93 level data analysis, integrate geospatial datasets, and draw conclusions. We discuss several
94 publicly available tools in DesignSafe and provide example queries to extract desired data, and
95 show examples of geospatial data integration.

96 **NGL DATABASE STRUCTURE**

97 The NGL database is a relational database, meaning that it has a well-defined data structure
98 and can be queried using structured query language (SQL). The term "database" is often
99 informally applied to file repositories lacking a formal organizational structure. In contrast, a
100 relational database is organized into a schema that describes the tables, fields, and relationships
101 among tables. In this context, a *table* is a collection of information containing a series of *fields*
102 (or columns). Database fields are related using keys. Every entry in the database is assigned a
103 *primary key* that uniquely identifies the field. In some cases, a field from one table might appear
104 in another table to relate the two tables. In this case, the primary key from the host table appears
105 as a *foreign key* in the other table to map the relationship.

106 The NGL database schema was developed over a number of years by a database working
107 group, and vetted by an interested community of geotechnical earthquake engineers through a
108 series of public workshops. Draft versions of the database were presented during workshops at
109 the University of California, Berkeley, in July 2017, and at the University of California, Los
110 Angeles in September 2018. The database schema presented here is the product of that process.
111 While the database structure is essentially complete, population of the database is ongoing and
112 is anticipated to continue indefinitely as additional data become available.

113 The NGL database consists of 60 tables that can be broadly categorized as: general, site,
114 event, and observation (Tables 1-4, respectively). The general tables contain fields about the
115 users, reviewers, project team members, and miscellaneous tables related to permissions,
116 password reset requests, and version logs. The general table also contains fields for file uploads
117 and citations of published datasets or other publications. The site tables contain
118 geotechnical/geological information such as CPT data, SPT data, soil layer descriptions (as in
119 borehole logs), geophysical measurements, laboratory tests, and groundwater table depth.
120 Geospatial data, such as geology maps, digital elevation models, etc. may also be included with
121 or linked to a specific site. The event tables contain information about the earthquake source,
122 recording stations, and ground motion intensity measures from recordings (if available). The
123 observation tables contain results of post-earthquake reconnaissance at the site, which may
124 include photographs, maps, measured ground deformations, commentary on the presence of
125 liquefaction surface manifestation or lack thereof, and links to large datasets such as light
126 detection and ranging (LIDAR), structure from motion (SfM), or geospatial raster files.

127

Table 1. General tables.

Table Name	Table Description	Number of Fields
CRES	Site creator	2
CREO	Observation creator	2
CRET	Test creator	2
DICT	Dictionary (service table)	7
FILE	Table storing supplemental files (16 MB max)	6
FILE_EXT	Table storing information about large supplemental files (>16 MB)	4
OBSM	Observation member information	3
OBSR	Observation Reviewer	3
password_resets	Password Reset	4
PERM	Permissions	5
phinxlog	Version log	5
CITATION	Citation for a publication	3
SITM	Site member information	3
SITR	Site Reviewer	3
TESM	Test member information	3
TESR	Test Reviewer	3
USER	User Information	14

129

130

131

132 **Table 2.** Site tables.

Table Name	Table Description	Number of Fields
BORH	General information for boreholes	11
DETL	Within-layer Description	4
GIND	Invasive Geophysical Investigation – Data	5
GINV	General information for geophysical investigation	7
GRAG	General information for particle size distribution test	4
GRAT	Particle Size Distribution – Data	4
GSWD	Surface Wave Geophysical Test – Dispersion Curve	5
GSWG	General information and configuration for surface wave geophysical test	7
INDX	Index Tests	9
ISPT	Standard Penetration Test Results	9
OTHF	Other Field Tests	7
OTHR	Other Laboratory Tests	6
PLAS	Atterberg Limits	6
RDEN	Relative Density	6
SAMF	Associated Files for Laboratory Tests	4
SAMP	General information for sample	11
SCPG	General information for Cone Penetration Test (CPT)	10
SCPT	Standard Penetration Test (SPT) – Data	6
SITC	Site Comments	5
SITE	Site general information	8
SITF	Junction table relating a file to a site	4
SITP	Junction table relating a publication citation to a site	4
SPEC	General information for specimens	7
STRA	Stratigraphic Layer Description	7
SWVD	Surface Wave Geophysical Test Data – V_s/V_p Profiles	7
SWVG	General Information for Surface Wave Geophysical Test	4
TEPT	Test Pit	8
TESC	Test Comments	5
TESF	Junction table relating a file to a test	4
TESP	Junction table relating a publication citation to a test	4
TEST	General information for in-situ tests	9
WATR	Ground water table information	5

133

134 **Table 3.** Event tables.

Table Name	Table Description	Number of Fields
EVNT	General information for earthquake events	20
GMIM	Ground Motion Intensity Measure recorded or estimated at a site	9
IM	Recorded Intensity Measure	125

SEGM	Fault Segments (finite fault models)	11
STAT	Recording stations	15

135

136 **Table 4.** Observation tables.

Table Name	Table Description	Number of Fields
FLDD	Displacement vectors	8
FLDF	Junction table relating a file to an observation	6
FLDP	Junction table relating a publication citation to an observation	4
FLDM	Liquefaction manifestation	11
FLDO	General information for field observation	6
OBSC	Observation Comment	5

137

138 A total of 494 different fields are contained within the tables defined by Tables 1 through
 139 4. A dictionary describing each individual field in these tables is provided in an interactive
 140 webpage: <http://nextgenerationliquefaction.org/schema/index.html>. The current schema at that
 141 web page is updated from an earlier version presented by Brandenberg et al. (2018), and any
 142 future changes will also be reflected in the online schema. Here we describe several example
 143 tables to illustrate key aspects of database functionality.

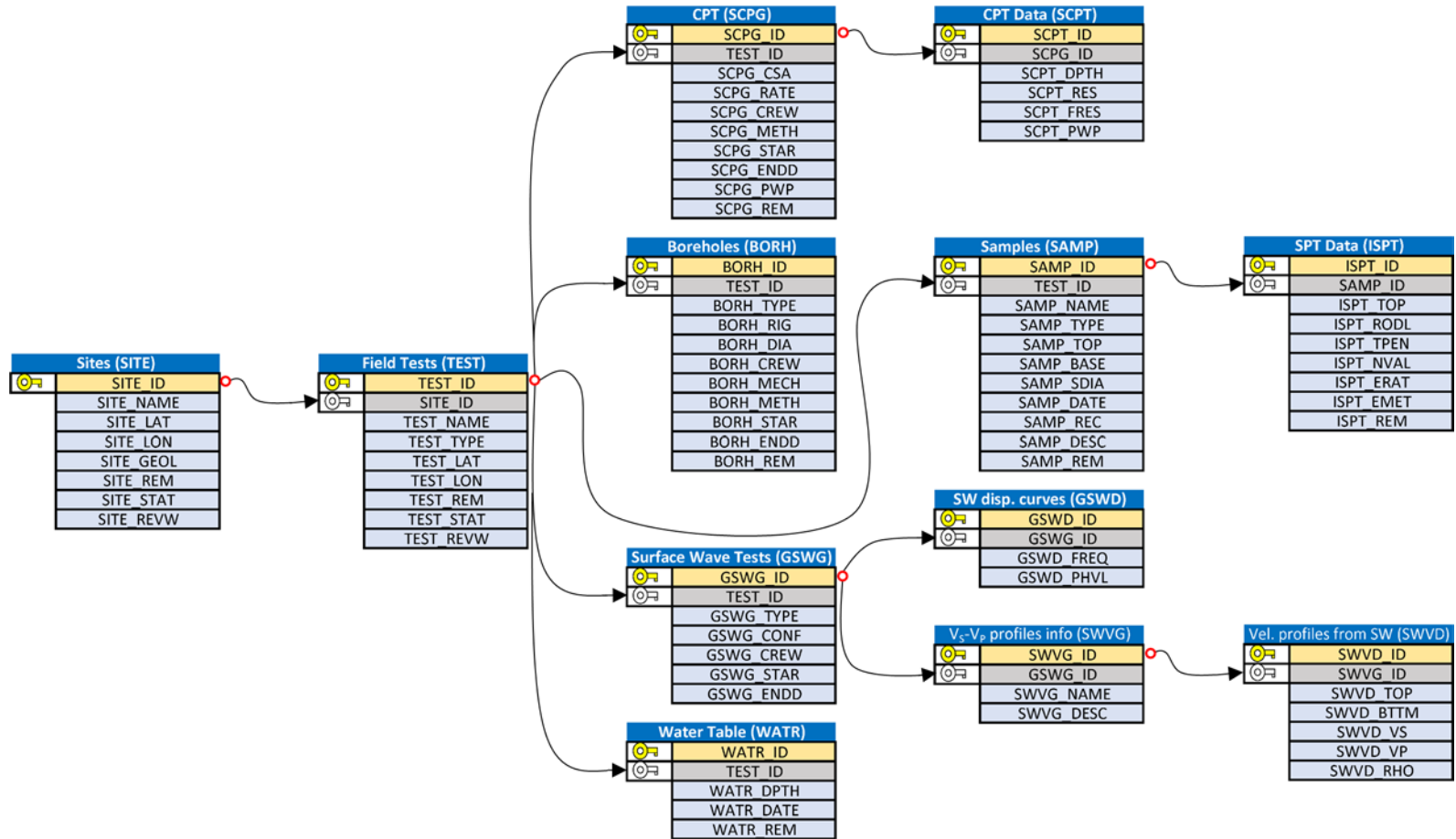
144 Figure 2 shows example site investigation tables and fields, with arrows indicating the
 145 primary key / foreign key relationships between tables. A site consists of a primary key
 146 (SITE_ID), site name (SITE_NAME), latitude (SITE_LAT), longitude (SITE_LON),
 147 description of surface geology (SITE_GEOL), a remark about the site (SITE_REM), a boolean
 148 field indicating whether the site has been submitted for review (SITE_STAT), and a boolean
 149 field indicating whether the site has been reviewed (SITE_REVW). Minimum data
 150 requirements for the SITE table are: SITE_NAME, SITE_LAT, and SITE_LON.

151 Because the NGL database scheme uses the word “site,” an operational definition is
 152 required. A site is a high level entity into which a team of NGL users organize their data. A
 153 site generally represents a contiguous geographical area that has been investigated by the team
 154 and for which observations of liquefaction effects have been made for an event or sequence of
 155 events. Latitude and longitude fields are required for each site so that the site can be located on
 156 the map within the GUI, but that does not mean that a site should be interpreted as a single
 157 location in space. Geotechnical conditions and observations of liquefaction effects may vary
 158 spatially within a site. Users must exercise judgment in assigning a specific geographical area

159 to a site, and are encouraged to provide a remark explaining their rationale for organizing the
160 information with a site.

161 Once a site has been established, a test or set of tests used to evaluate site conditions may
162 be defined for that site. Note that the TEST table has a SITE_ID field, which is a foreign key
163 that links the TEST table with a particular SITE. In the TEST table TEST_NAME,
164 TEST_TYPE, TEST_LAT, and TEST_LON are required fields. In this manner, multiple tests
165 may be specified for a specific site without the need for repeating information from the site
166 table. The types of tests illustrated in Figure 2 include CPT (SCPG), borehole (BORH), surface
167 wave geophysical test (GSWG), groundwater table measurement (WATR), and sample
168 (SAMP). As shown in Figure 2, an individual test has a location, which does not necessarily
169 align with that of the SITE. Although not shown in Figure 2, additional test types, including
170 stratigraphy (STRA), detailed soil description (DETL), test pit (TEPT), and invasive
171 geophysical tests (GINV), may also be provided. Furthermore, users may upload source
172 materials such as PDF files, photos, maps, etc. as Binary Large Object (BLOB) files. We limit
173 BLOB file size to 16 MB because large files could slow operation of the database and GUI.
174 When a user wishes to include a file larger than 16 MB in the site data, the large data files must
175 be published outside of the NGL database and assigned a digital object identifier (DOI). The
176 DOI for the published data may then be included with the NGL database site data using the
177 CITATION and FILE_EXT tables. We require that external files be published and assigned a
178 DOI to maintain integrity of the data, and ensure that the URL created by appending the DOI
179 to <http://doi.org/> will always point to the correct data location. For example, the NGL website
180 can be found at <http://doi.org/10.21222/C2J040>, and will always be accessible through this
181 DOI even if the host location of the website changes.

182



183

184

Figure 2. Subset of NGL relational database schema illustrating tables containing site investigation data.

185 For CPT data, the SCPG table contains general information about the test, including the
186 cone area (SCPG_CSA), push rate (SCPG_RATE), crew (SCPG_CREW), method
187 (SCPG_METH) (e.g., ASTM D5778-12), time stamp at the start and end of the test
188 (SCPG_STAR and SCPG_ENDD, respectively), position of the pore pressure measurement
189 (SCPG_PWP), and remarks (SCPG_REM). The CPT data are contained in the SCPT table,
190 which has SCPG_ID as a foreign key. The fields include depth (SCPT_DPTH), tip resistance
191 (SCPT_RES), sleeve friction (SCPT_FRES), and pore pressure (SCPT_PWP). Minimum data
192 requirements for the SCPT table are: SCPT_DPTH and SCPT_RES.

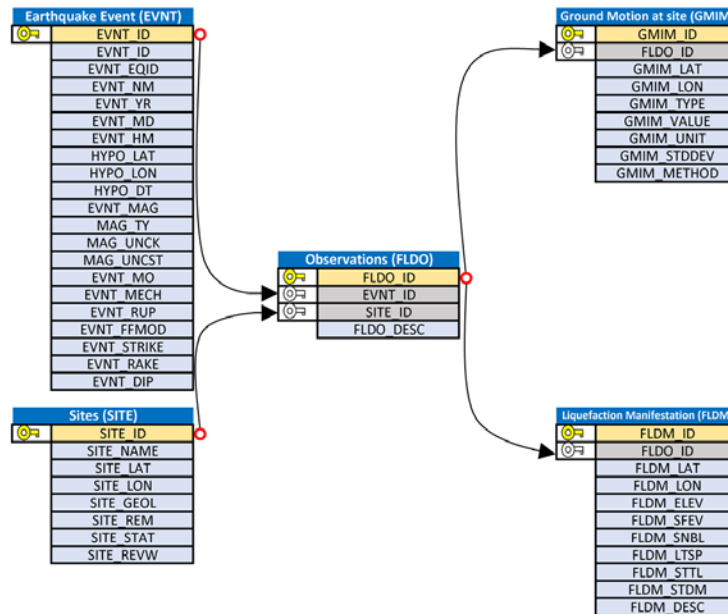
193 For SPT data, users enter borehole information in the BORH table such as borehole type,
194 rig, diameter, crew, hammer drop mechanism, start and end dates. Users then also enter
195 information about the samples in the SAMP table, including the sampler type, diameter, and
196 depth of the top and bottom of the sample. SPT blow count data are entered in the ISPT table,
197 which contains SAMP_ID as a foreign key. Users can enter the distance that the sampler was
198 driven, the number of blows required to drive it that distance, hammer energy ratio, method
199 used to obtain hammer energy ratio (i.e., directly measured, calibrated rig, hammer type), and
200 rod length.

201 Figure 2 also shows the tables for surface wave measurements. In this case, users upload
202 general information about the surface wave measurements in the GSWG table, and the surface
203 wave dispersion curve data in the GSWD table. A velocity profile, or multiple velocity profiles,
204 obtained by inversion of the measured dispersion curve may also be uploaded in the SWVG
205 and SWVD tables. We consider a velocity profile from a surface wave measurement to be
206 subjective because the inversion procedure is highly non-unique and many different velocity
207 profiles may provide a good fit to a measured dispersion curve (e.g., Foti et al., 2018).
208 However, the measured dispersion curve is relatively objective, and therefore the dispersion
209 curve should be included in the database when possible.

210 Figure 3 illustrates tables associated with observations of liquefaction manifestation or lack
211 thereof. Observations are first organized into a junction table, FLDO, that contains the
212 observation primary key, and foreign keys for SITE_ID and EVNT_ID. These foreign keys
213 must be present because they connect the observation to the site and event for which the
214 observation was made. A general description of the observation at the site for the event should
215 be provided (FLDO_DESC). In some cases, an observation is made after a sequence of events
216 and it is not clear the extent to which each event contributed to the observation. In this case,

217 users must use judgment in selecting an event, and are encouraged to explain this in the
218 FLDO_DESC field. The ground motion intensity measure for traditional triggering procedures
219 has been peak horizontal acceleration (PGA), although other intensity measures, such as peak
220 ground velocity, peak ground displacement, 5%-damped pseudo-spectral acceleration for a
221 range of oscillator periods, significant duration, Arias intensity, and cumulative absolute
222 velocity above 5 cm/s^2 (CAV₅, Kramer and Mitchell 2006), can also be input. The method
223 used to estimate the intensity measure (GMIM_METHOD) is a required field, and can be
224 accompanied by a standard deviation (GMIM_STDDEV) representing uncertainty in the
225 estimate. Quantifying uncertainty is important because we envision three scenarios for ground
226 motion estimation, in order of increasing uncertainty:

- 227 (i) A strong motion record is co-located with a liquefaction observation. Uncertainty
228 is minimized in this case. Currently 23 such sites are available in the NGL database,
229 which have produced 31 total observations. Procedures described by Kramer et al.
230 (2016) and Greenfield (2017) identify the timing of liquefaction triggering from
231 waveforms.
- 232 (ii) The event is recorded by a network of strong motion stations, but a strong motion
233 record is not co-located with the liquefaction observation. In this case, spatial
234 interpolation techniques can be utilized, ideally with consideration of differences in
235 site conditions at the liquefaction observation site relative to the recording stations
236 [e.g., Stafford (2012); Kwak et al (2016)].
- 237 (iii) Strong motion records are sparse or non-existent for a particular event, and shaking
238 intensity is estimated using a ground motion model. This approach involves
239 significant uncertainty and judgment, but is frequently required for case histories
240 used in previous susceptibility, triggering, and/or consequences models.



241

242 **Figure 3.** Subset of NGL relational database schema illustrating tables containing event data.

243

244 Users may describe detailed observation(s) of site performance using the FLDM table. The
 245 location of the observation is indicated by the FLDM_LAT, FLDM_LON, and FLDM_ELEV
 246 fields. The FLDM_SFEV field indicates whether there is surface evidence of liquefaction (0 =
 247 no, 1 = yes). It is important to note that FLDM_SFEV = 0 indicates that an observation was
 248 made, and surface evidence was confirmed to have not occurred. A lack of surface evidence
 249 does not necessarily indicate a lack of liquefaction at some depth within the soil profile.
 250 Additional fields include evidence of sand boils (FLDM_SNBL), lateral spreading
 251 (FLDM_LTSP), settlement (FLDM_STTL), and structural or foundation damage
 252 (FLDM_STDM). Additional data entry options include descriptions of observations, ground
 253 displacement vectors uploaded using the FLDD table, and files such as photographs and maps
 254 of observations of damage uploaded using the FILE and FLDF tables. Minimum data
 255 requirements for the FLDM table are: FLDM_LAT, FLDM_LON, FLDM_SFEV,
 256 FLDM_SNBL, FLDM_LTSP, FLDM_STTL, and FLDM_STDM.

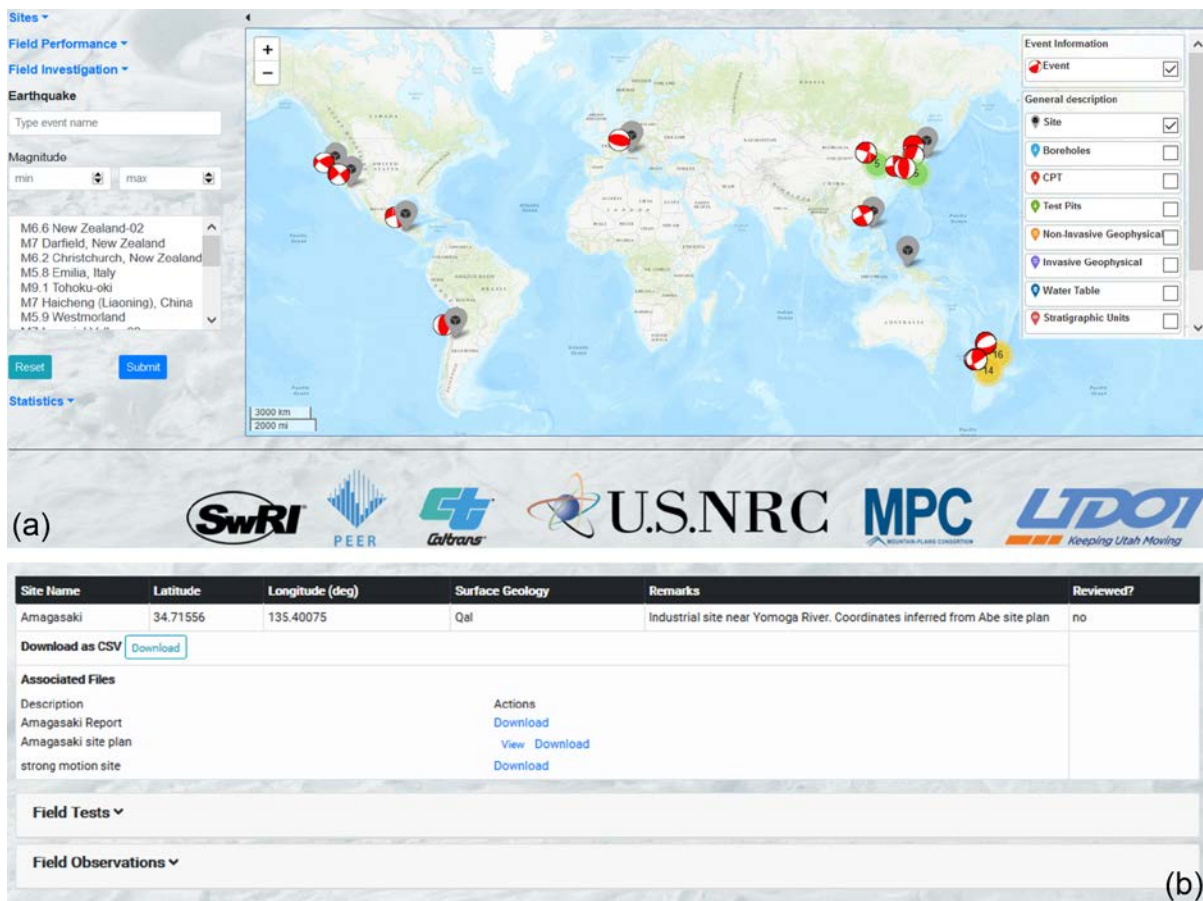
257

GRAPHICAL USER INTERFACE

258 The web GUI was developed using PHP: Hypertext Preprocessor, Hypertext Markup
 259 Language 5, Javascript, and Cascading Style Sheets within the CakePHP web framework. The
 260 GUI also utilizes two Application Program Interfaces (API's) to organize the data geospatially:
 261 the Environmental Systems Research Institute Arc Geographic Information System API and

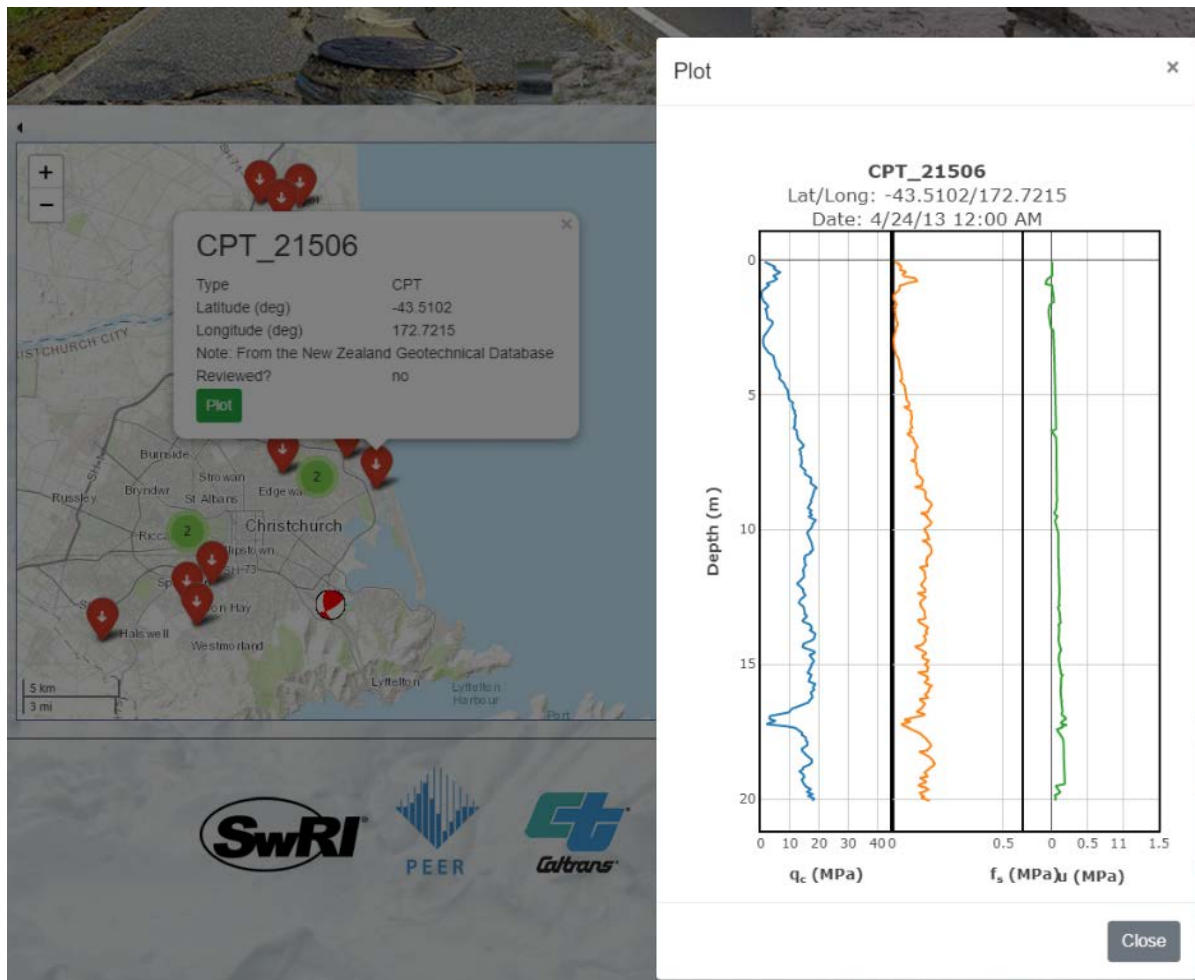
262 the Leaflet Javascript API. The GUI can be used to visualize, upload, and download
 263 liquefaction case history data. The homepage of the database provides an overview of the
 264 geographic distribution of events, sites, and observations (Figure 4). The NGL database GUI
 265 also allows users to interact with the data by means of a list view (Figure 4b), which is
 266 convenient for seeing all of the data fields for a particular site, event, or observation in tabular
 267 form.

268 In map view, users can utilize the left panel to filter the data based on earthquake name,
 269 magnitude range, or by selecting specific events from the event list. Although not shown in
 270 Figure 4, the left panel also enables filtering data based on field performance by including or
 271 excluding sites that exhibited surface evidence, sand boils, lateral spreading, settlement, and/or
 272 structural damage. Case histories can also be filtered based on available field investigation
 273 information, including boreholes, CPTs, test pits, geophysical tests, and other tests. The right
 274 panel provides viewing options, including the ability to show or hide various database objects,
 275 and to change the map view to topographic (default), imagery, or terrain.



276 **Figure 4.** (a) Homepage of the NGL database GUI (map view); and (b) organized list of case histories
 277 in the database (list view).
 278

280 Users may view site, event, and observation data through the GUI, as illustrated in Figure
281 5, which shows results from a cone penetration test (CPT_21506) performed in Christchurch,
282 New Zealand after the Canterbury earthquake sequence. The plot shows measured cone tip
283 resistance, sleeve friction, and pore pressure. The figure is not stored in the database as an
284 image, but rather is generated from the data when a user clicks the "Plot" button. This prevents
285 potential inconsistencies between the data stored in the database and the figure. In a similar
286 manner, users can plot borehole data, including stratigraphic details and SPT blow counts,
287 shear wave velocity profiles (and dispersion curves for surface wave measurements), and
288 observations of earthquake damage including photographs, maps, and damage descriptions.



289
290 **Figure 5.** Screenshot of NGL GUI showing CPT data for CPT_21506 in Christchurch, New Zealand.
291

292

DATA REVIEW PROCESS AND QUALITY CONTROL

293

294

295

296

297

298

299

300

301

302

303

304

305

306

307

All data uploaded to the NGL database is reviewed using tools incorporated within the GUI. The NGL Database Working Group provides oversight to the review process. The goals of the review are to (i) ensure consistency between uploaded information and source documents, (ii) verify that all required fields are provided, (iii) identify ambiguities, or items that require clarification, and (iv) check for reasonableness of data to identify errors in data entry such as incorrect unit conversions, inappropriate negative values, etc. The review is intended to be objective; subjective opinions are not part of the review process. For example, a reviewer is justified in requesting clarification when data uploaded to the database does not agree with the same data plotted in a publication. On the other hand, a reviewer may believe that SPT data without hammer energy ratio measurements are not valuable and should not be included in development of a liquefaction model. However, the reviewer cannot decline the data based on this subjective opinion. The NGL project has been structured in such a way that subjective judgments of this type are not made during database development, instead being reserved for the model development phase. Two independent reviewers must formally review each individual piece of information uploaded to the database.

308

309

310

311

312

313

314

315

316

317

318

319

320

Database population is usually performed in two-steps. During the first step, users and research teams upload data, which is flagged as un-submitted and un-reviewed, and is only available to project team members in the NGL GUI. Once the user or team believes the data is ready, they submit it to the review team, at which point the data is flagged as submitted, but un-reviewed and is made available to all NGL users through the NGL GUI. After all components of a case history have been reviewed and accepted, the case history is flagged as reviewed. At this stage, users may request a DOI for their dataset. A case history is complete only if includes at least the minimum required data components, and the original source of each individual piece of information is provided. Source documents are often journal or conference publications, technical reports, theses or dissertations. It is also possible for users to upload original (not previously published) data for which the source documents can be given as field and/or laboratory minutes or notes. In such cases, the assignment of a DOI is recommended to associate the data with the user.

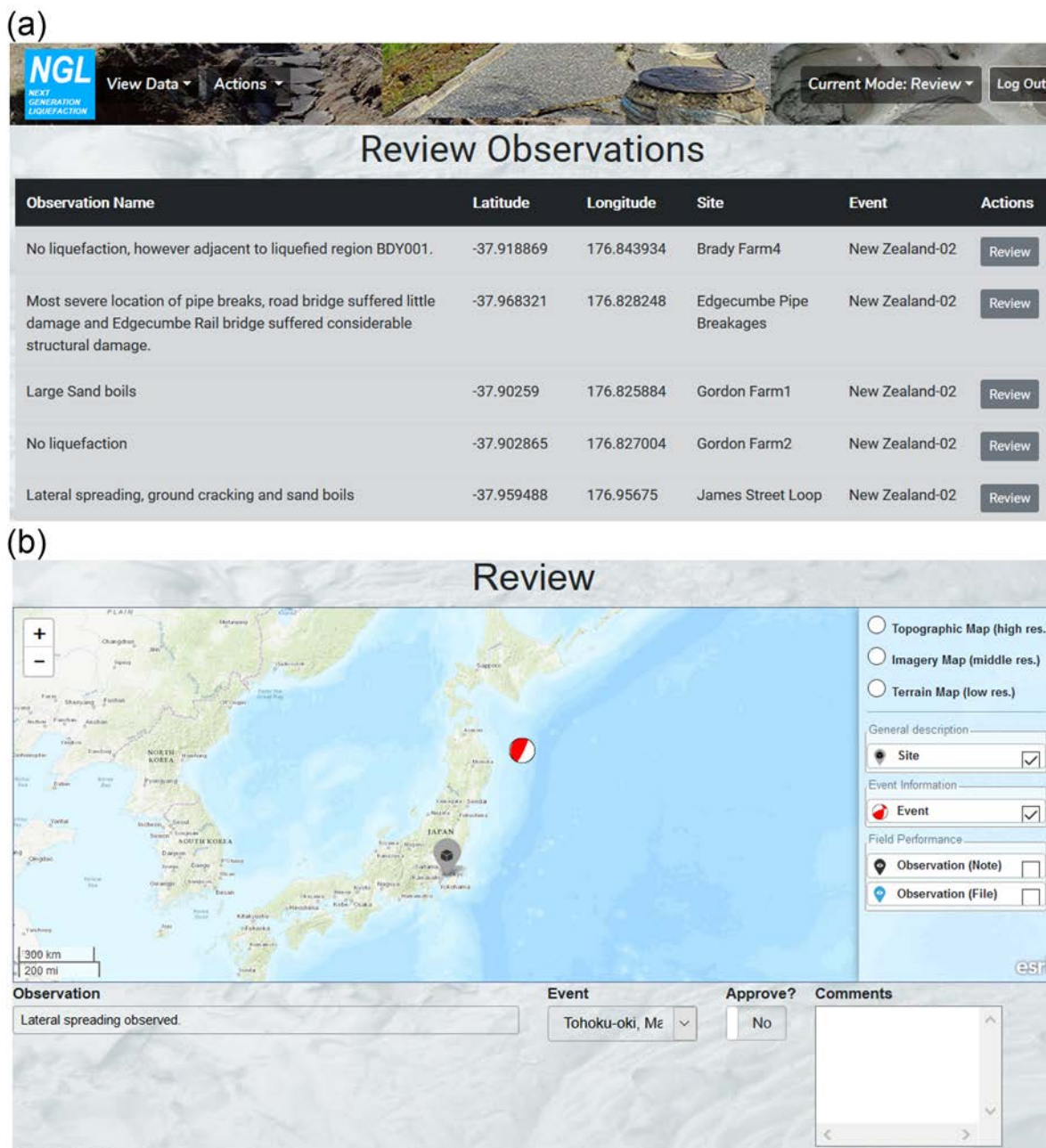
321

322

323

Within the NGL GUI, review functions are only accessible to users having appropriate permissions. As a result, regular users are not able to access the review section of the GUI. Case history components are reviewed using three separate panels in the NGL GUI. Figure 6a

324 shows a list of post-earthquake observations under review, while Figure 6b shows the review
 325 form for a specific observation entry in the NGL database. Similar forms are available for site
 326 information and field investigation data. The review process for an example case history and
 327 additional information on the quality control process implemented in the NGL project are
 328 provided by Zimmaro et al. (2019b).



329 **Figure 6.** (a) Review observation panel showing post-earthquake observations under review; (b) review
 330 form for post-earthquake observations.
 331

332

CLOUD-BASED DATABASE INTERACTION VIA DESIGNSAFE

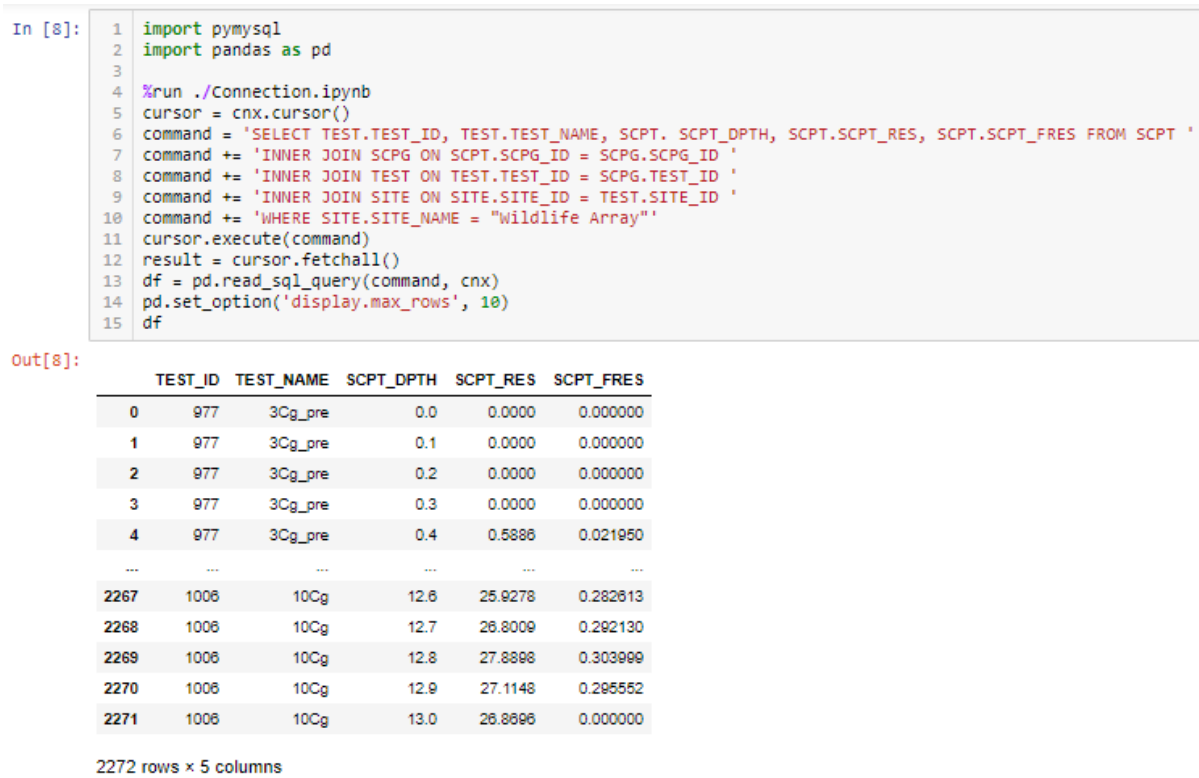
333 The NGL database GUI allows users to upload, visualize, and download data from the NGL
334 database, but users cannot use the GUI to perform calculations on the data. If, for example, a
335 user wished to compute a liquefaction index such as LPI_{ISH} (Maurer et al. 2015) for a specific
336 CPT sounding, or perform geospatial liquefaction analysis (e.g. Zhu et al. 2015, 2017) they
337 could not do so through the GUI. One option for such analyses is to download CPT data and
338 perform calculations on local computers. However, we anticipate that the size of the database
339 will eventually render this approach infeasible.

340 To permit users to interact with the NGL database in the cloud, and integrate the NGL data
341 into their custom workflows, we periodically replicate the NGL database in DesignSafe. The
342 significance of this replication is that users can interact with the DesignSafe version of the
343 database via applications available through the DesignSafe Discovery Workspace, such as
344 Jupyter notebooks, QGIS, and the Potree point cloud viewer. A Jupyter notebook is a server-
345 client application that allows editing and running notebook documents via a web browser. It
346 combines rich text elements (equations, figures, HTML, LaTeX) and computer code executed
347 by a Python kernel (Perez and Grainger 2007). These Jupyter notebooks utilize Python libraries
348 for performing SQL queries to extract data from the database, where the extracted data may
349 then be processed using custom computer code. Five example Jupyter notebooks that perform
350 basic tasks that we anticipate users might perform during model development have been
351 published in DesignSafe. One notebook provides example queries that extract various data into
352 tables (Brandenberg and Zimmaro, 2019a, DOI: 10.17603/ds2-xvp9-ag60.). Notebooks are
353 also available for viewing CPT (Brandenberg and Zimmaro, 2019b, DOI: 10.17603/ds2-99kp-
354 rw11), boring logs and SPT (Lee et al., 2019, DOI: 10.17603/ds2-sj7t-av93), and invasive and
355 non-invasive geophysical tests (Zimmaro and Brandenberg, 2019, DOI: 10.17603/ds2-tq39-
356 kp49 and Brandenberg and Zimmaro, 2019c, DOI: 10.17603/ds2-cmn0-h864).

357 Example SQL Queries

358 Figure 7 shows an example SQL query that extracts CPT data at the Wildlife Array site.
359 The query is actually a single text string, but is broken into five lines here for clarity. The query
360 begins on Line (6) of the Jupyter notebook, where the SELECT command queries TEST_ID,
361 TEST_NAME, SCPT_DPTH, SCPT_RES, and SCPT_FRES. Note that data is queried from
362 two different tables (TEST and SCPT), and the table name is prepended to the field name with
363 a "." separator. Line (7) utilizes an INNER JOIN command, which synthesizes two tables into

364 a single table based on a common shared key. In this case, the SCPT and SCPG tables are
 365 combined based on a common value of SCPG_ID, which is the primary key for SCPG and a
 366 foreign key for SCPT. In line (8) another INNER JOIN adds the TEST table based on the
 367 TEST_ID key, and in line (9) the final INNER JOIN adds the SITE table based on the SITE_ID
 368 key. In line (10), the WHERE statement indicates that the requested data should be included in
 369 the query result for sites where SITE_NAME = 'Wildlife Array'. The output from the query
 370 shown in Figure 7 is a small excerpt of the overall resulting data table. Note that different CPT
 371 soundings are indicated by different TEST_ID values.



372
 373 **Figure 7.** Example SQL query to extract CPT data from Wildlife Array site, and output table showing
 374 truncated result.

375
 376 Figure 8 shows an example query of Event and Observation data for the Wildlife Array
 377 site. In this case, the query extracts earthquake magnitude (EVNT_MAG), name
 378 (EVNT_NAME), and year (EVNT_YEAR), along with observation latitude (FLDM_LAT),
 379 longitude (FLDM_LON), whether surface evidence of liquefaction was observed
 380 (FLDM_SFEV), and a description of the observation (FLDM_DESC). Observations are
 381 available at the Wildlife Array site for four different events, two of which produced surface
 382 evidence of liquefaction (1981 M5.9 Westmorland and 1987 M6.54 Superstition Hills-02) and

383 two of which produce no surface evidence (1987 M6.2 Superstition Hills-01 and 2010 M7.2
 384 El Mayor-Cucapah).

```
In [1]: 1 # Imports libraries and modules
        2 import pymysql
        3 import pandas as pd
        4
        5 # Establishes connection to the NGL database
        6 *run ./Connection.ipynb
        7 cursor = cnx.cursor()
        8
        9 command = 'SELECT EVNT_MAG, EVNT_NM, EVNT_YR, FLDM.FLDM_LAT, FLDM.FLDM_LON, FLDM.FLDM_SFEV, FLDM.FLDM_DESC FROM FLDO '
       10 command += 'INNER JOIN FLDM ON FLDO.FLDO_ID = FLDM.FLDM_ID '
       11 command += 'INNER JOIN EVNT ON EVNT.EVNT_ID = FLDO.EVNT_ID '
       12 command += 'INNER JOIN SITE ON FLDO.SITE_ID = SITE.SITE_ID '
       13 command += 'WHERE SITE_NAME = "Wildlife Array"'
       14
       15 cursor.execute(command)
       16 result = cursor.fetchall()
       17 df = pd.read_sql_query(command, cnx)
       18 pd.set_option('display.max_colwidth', 100)
       19 df
```

Out[1]:

	EVNT_MAG	EVNT_NM	EVNT_YR	FLDM_LAT	FLDM_LON	FLDM_SFEV	FLDM_DESC
0	5.90	Westmorland	1981	33.0976	-115.5306	1	Significant liquefaction was observed at many locations within the Imperial Valley. Bennett et ...
1	6.22	Superstition Hills-01	1987	33.0976	-115.5306	0	Holzer et al. (1989) indicates the piezometers installed by Bennett et al. (1984) showed no evid...
2	6.54	Superstition Hills-02	1987	33.0976	-115.5306	1	Superstition Hills Earthquake observations by Holzer et al. (1989)
3	7.20	El Mayor-Cucapah	2010	33.0976	-115.5306	0	No observed liquefaction manifestation. This is also confirmed by co-located piezometric recordi...

385
 386 **Figure 8.** Example SQL query to extract Event and Observation data from Wildlife Array site, and
 387 output table showing truncated result.

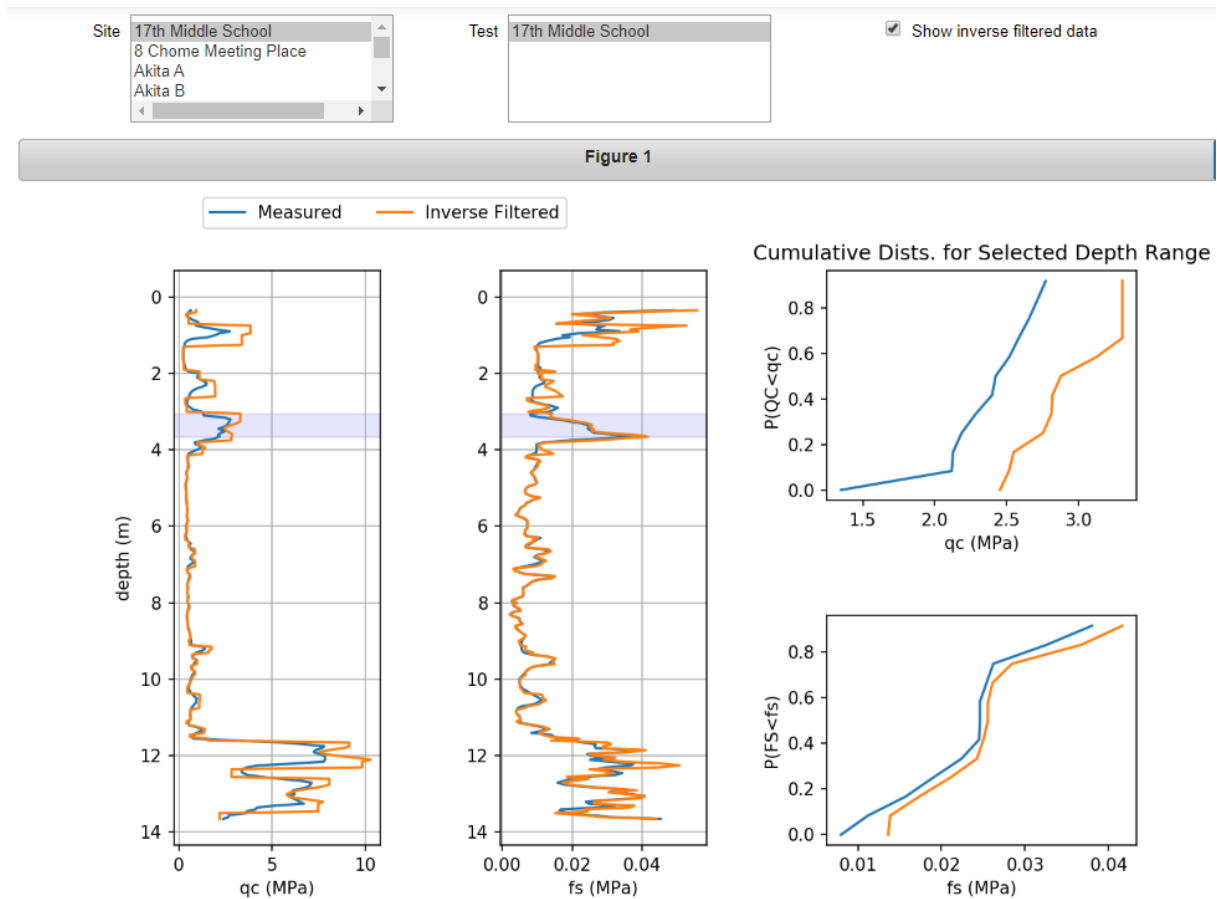
388

389 Visualization Tools for Geotechnical Site Investigation Data

390 Figure 9 shows a Jupyter notebook for visualizing CPT data. Users select a site from a
 391 dropdown menu, and the tool populates the *Test* box with CPT profiles for that site. The script
 392 used to create this tool combines SITE and SCPT table entries using the INNER JOIN
 393 command. It facilitates visualization of cone tip resistance (q_c) and sleeve friction (f_s) for CPT
 394 profiles, along with cumulative distribution functions (CDFs) for user-specified depth ranges
 395 (full-profile or narrower depth intervals). On the right side of the visualization panel, a box
 396 labelled 'Show inverse filtered data' provides a filtered q_c profile based on the Boulanger and
 397 DeJong (2018) procedure. This feature is useful for analyzing profiles with thinly-interbedded
 398 soils.

399 Figure 10 shows a tool developed to visualize boring logs and SPT data. This tool allows
 400 users to select a site from a dropdown menu only populated with sites having boring logs and/or
 401 SPT data. This tool combines SITE, STRA, and ISPT tables data entries using the INNER
 402 JOIN command. After selecting a site, the tool automatically populates the *Remarks* field
 403 (which shows available remarks for that site) and the *TEST* box with all available boring logs
 404 and SPT profiles for the site. After selecting a test, the tool plots SPT profiles (N-value versus

405 depth) and boring logs side-to-side on the same vertical scale. The tool also plots the CDF for
406 SPT data over user-specified depth ranges. Two additional visualization tools are available on
407 DesignSafe: (1) a tool showing dispersion curves and inverted V_s profiles (if available) for
408 non-invasive geophysical tests (i.e. surface wave methods), and (2) a tool showing shear wave
409 velocity profiles and CDFs from invasive geophysical tests (e.g., cross hole, down hole, and
410 suspension logging). The visualization tool for non-invasive geophysical tests combines SITE,
411 GSWG, GSWD, SWVG, and SWVD table entries, while the visualization tool for invasive
412 geophysical tests combines SITE and GIND table entries. In both cases table entries are
413 combined using the INNER JOIN command.



414

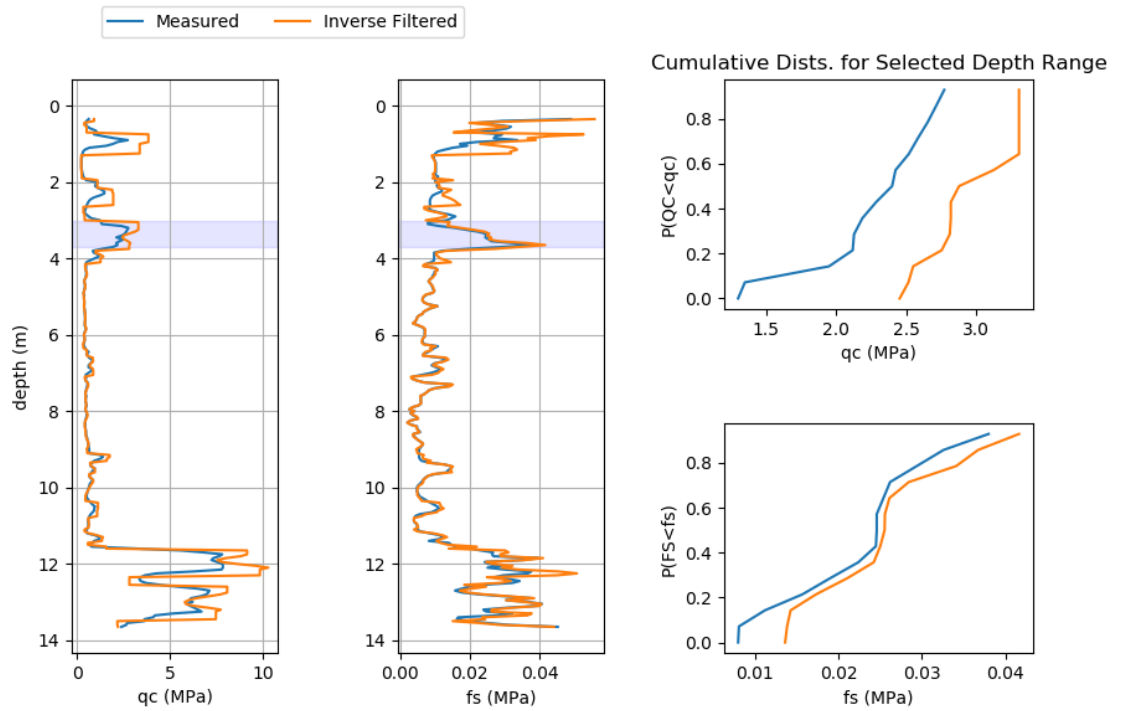
415

Site: 17th Middle School
 Alameda Naval Air Station
 Awaroa Farm
 Barrington
 Bonds Corner

Test: 17th Middle School

Show inverse filtered data

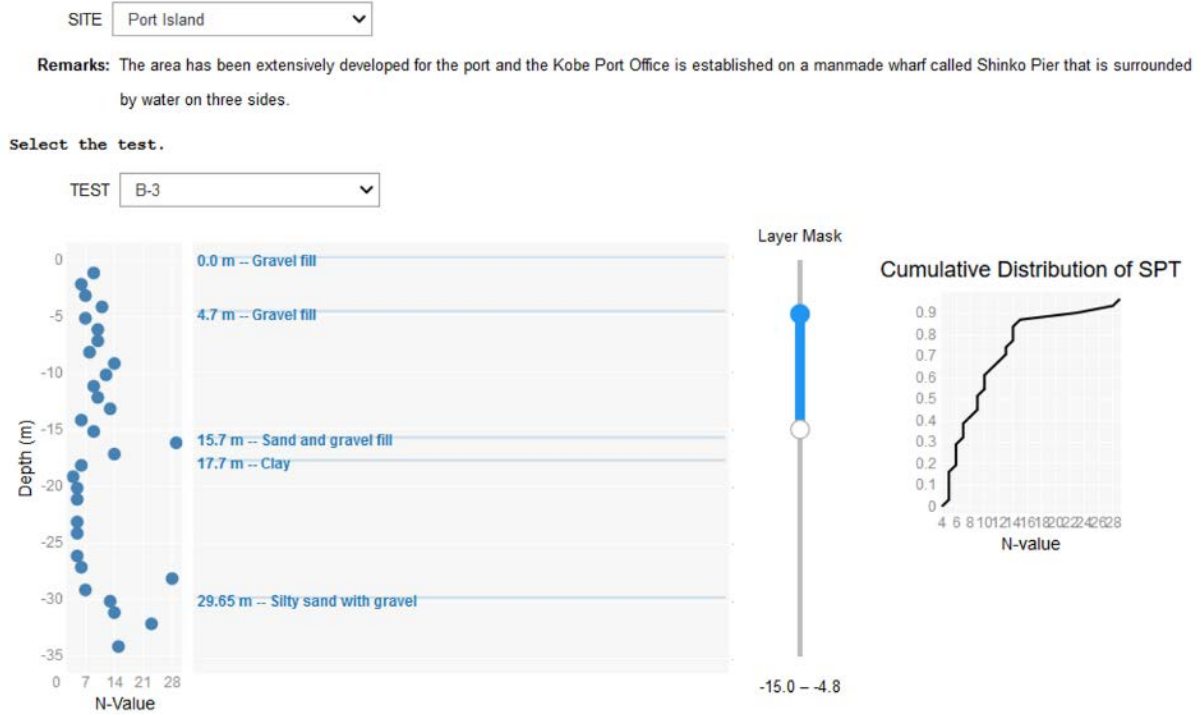
Figure 1



416

417

Figure 9. Output from the NGL CPT viewer available on DesignSafe.



418

419

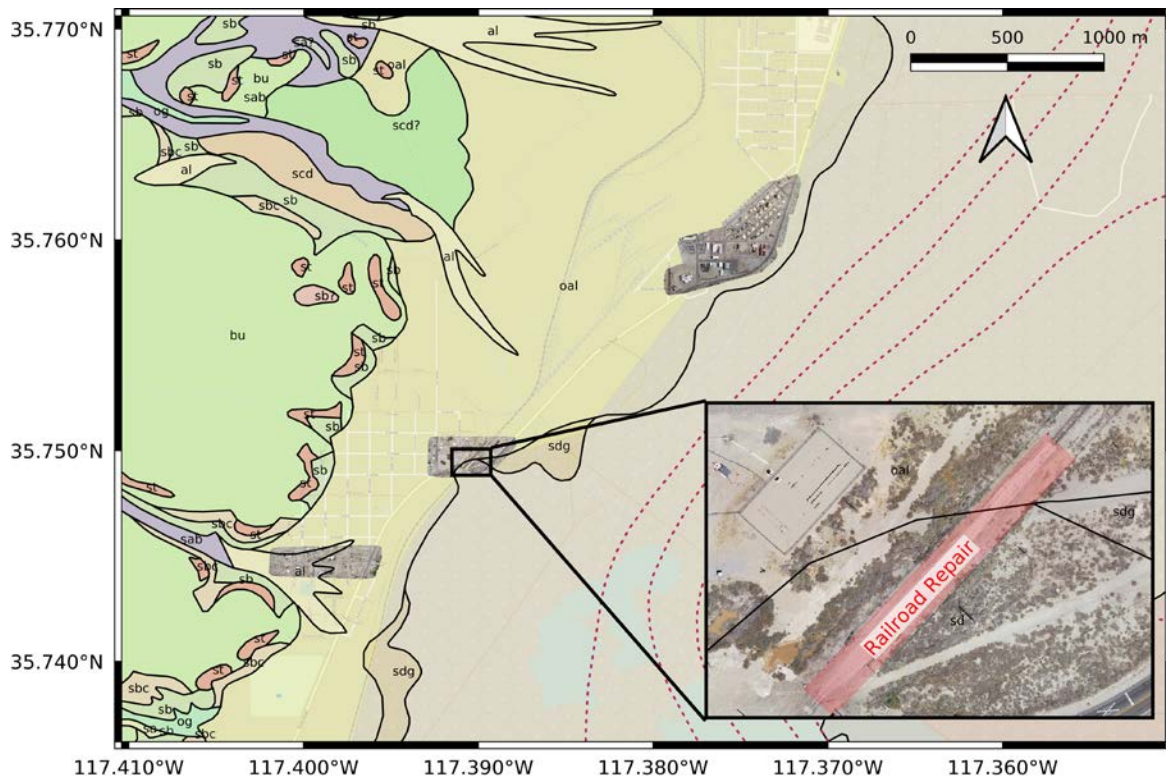
420

Figure 10. Output from the NGL SPT viewer available on DesignSafe.

421 **Visualization Tools for Geospatial Data**

422 Observations of liquefaction manifestation are increasingly utilizing techniques such as LIDAR
423 (e.g. Olsen et al., 2012; Imakiire and Koarai, 2012; Konagai et al., 2013; and Rathje et al., 2017), SfM
424 applied to digital photos collected using unmanned aerial vehicles (UAV's) (e.g. Franke et al., 2017;
425 Stewart et al., 2019; and Winters et al. 2019), and correlation analysis of satellite images (Rathje et
426 al., 2017). Furthermore, geospatial products such as maps of surface geology, bodies of water, and
427 digital elevation models provide useful information for liquefaction triggering evaluation, and have
428 been used to supplement geotechnical data in regional liquefaction assessment procedures (e.g., Zhu
429 et al. 2015, 2017). These geospatial data objects are important to include in the NGL database..

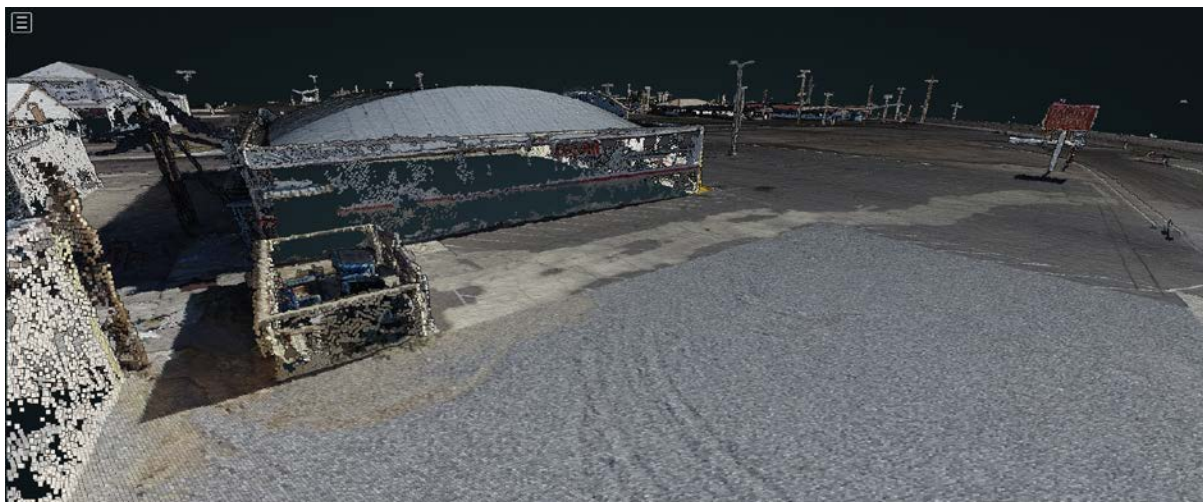
430 An example application of linking geospatial data with NGL data is provided for observations in
431 Trona and Argus after the 2019 Ridgecrest earthquake sequence. A Geotechnical Extreme Events
432 Reconnaissance Association (GEER) reconnaissance team visited these sites after the earthquakes
433 (Stewart et al. 2019) to perform ground-based observations using GPS trackers, digital cameras, and
434 hand-held measuring devices, and subsequently a team visited these sites to fly UAV's and gather
435 image data. Data from these reconnaissance missions was published in DesignSafe (Brandenberg et
436 al. 2019 and Winters et al. 2019), and assigned DOI's that are included as citations in the CITATION
437 table and linked to the observation through the FLDP table. Orthomosaic images obtained from the
438 UAV survey (Winters et al. 2019) are superposed on a surface geology map (Smith 2009) using QGIS
439 in DesignSafe in Figure 11. Three different orthomosaics are shown, and a zoomed-in view of one
440 orthomosaic shows a railroad that required repair due to liquefaction effects near the intersection of
441 three different geologic units [sdg (gravel and sand), oal (older alluvium), and sd (sand and silt)].



442

443 **Figure 11.** Map of Trona and Argus where liquefaction effects were observed after the Ridgecrest
 444 earthquake sequence. The map includes orthomosaic images obtained from UAV SfM surveys (Winters
 445 et al. 2019), and a surface geology map by Smith (2009).

446 A point cloud generated by SfM processing of the UAV images shows surface evidence of
 447 liquefaction at the site of the Family Dollar store in Trona, CA in Figure 12. The image is a
 448 screenshot from the Potree point cloud viewer available in DesignSafe. Sand ejecta originating
 449 from a utility pole near the left side of the image flowed over the gravel and parking lot toward
 450 the sign on the right of the image.



451

452 **Figure 12.** Point cloud from SfM processing of UAV images at the Family Dollar building in Trona,
453 CA (Winters et al. 2019).

454

CONCLUSION

455 In this paper we present the Next Generation Liquefaction (NGL) database (Zimmaro et al.
456 2019a, DOI: 10.21222/C2J040). The NGL database is an open-source tool that results from a
457 multi-year, ongoing community effort. We describe the NGL database organizational structure
458 (i.e. the schema describing relationships among tables) and provide information about selected
459 tables in the database, including minimum data requirements. The NGL database contains
460 objective information about liquefaction, or lack thereof, during past earthquake events. Each
461 individual site and observation component is reviewed through a formal vetting process
462 coordinated by the NGL Database Working Group.

463 The NGL database is accessible through a GUI that allows users to upload, visualize, and
464 download data. The database is also replicated onto DesignSafe where users can write queries
465 and utilize Jupyter notebooks to interact with the data in the cloud, and integrate geospatial
466 data into their workflow. We envision these cloud-based tools to be particularly useful for data
467 analysis in support of development of future liquefaction susceptibility, triggering, and
468 consequences models.

469

ACKNOWLEDGEMENTS

470 Financial support for the NGL project is provided by California Department of
471 Transportation (Caltrans) through the Pacific Earthquake Engineering Research Center
472 (PEER), and by the U.S. Nuclear Regulatory Commission (NRC) through the Southwest
473 Research Institute (SWRI). Neither the U.S. Government nor any agency thereof, nor any of
474 their employees, makes any warranty, expressed or implied, or assumes any legal liability or
475 responsibility for any third party's use, or the results of such use, of any information, apparatus,
476 product, or process disclosed in this paper, or represents that its use by such third party would
477 not infringe privately owned rights. The views expressed in this paper are not necessarily those
478 of the U.S. Nuclear Regulatory Commission. The authors acknowledge the contributors of
479 datasets, input on the schema during workshops, and/or input during database working group
480 meetings by: Russel Green and Kristin Ulmer (Virginia Tech), Ross Boulanger (UC Davis),
481 Robert Kayen (USGS/UC Berkeley), Kyle Rollins (BYU), Sjoerd van Ballegooy and Mike Liu
482 (Tonkin + Taylor), Mike Greenfield (Greenfield Geotechnical), Christine Beyzaei and Sean

483 Ahdi (Exponent), Jonathan Bray (UC Berkeley), James Gingery (Hayward Baker), Eric
484 Thompson (USGS), Yousef Bozorgnia (UCLA), Miriam Juckett, (SwRI), Roy Mayfield
485 (Consulting Engineer), Steve Bartlett and Massoud Hosseinali (University of Utah), Mahyar
486 Sharifi-Mood, Tim Cockerill, Christopher Jordan, Steve Mock (Texas Advanced Computing
487 Center), Ellen Rathje, Maria Giovanna Durante, and Michael Little (University of Texas),
488 Laurie Baise (Tufts University), Silas Nichols (FHWA), Derrick Wittwer (Bureau of
489 Reclamation), Ahmed Elgamal (UCSD), Lelio Mejia (Geosyntec), Robert Pyke (Consulting
490 Engineer), Albert Kottke (PG&E), Yi Tyan Tsai (GeoEngineers Inc.), Tom Shantz (Caltrans),
491 Zia Zafir (Kleinfelder), Esam Abraham (Southern California Edison), Khaled Chowdhuri
492 (USACE), Harold Magistrale (FM Global), Marty Hudson (Wood), Jianping Hu (LADWP),
493 Craig Davis (recently retired LADWP), Joseph Weber (Loyola Marymount University), Tim
494 Ancheta (RMS), Ariya Balakrishnan (California Division of Safety of Dams), and Allison Lee,
495 Honor Fisher, Omar Issa, Wyatt Iwanaga, Arielle Sanghvi, Christopher Nicas, Jared Rivera,
496 Michael A. Winders, Naoto Inagaki, Sahil Sibal, Siddhant Jain, Trini Inouye, Bryan Ong,
497 Anjali Swamy, Tristan Buckreis, and Chukwuebuka Nweke (UCLA). The web-based graphical
498 user interface was developed by Joey Mukherjee, Zachary Murphy, and Steven Ybarra
499 (SWRI).

500

REFERENCES

- 501 Andrus, R. D. and Stokoe II, K. H., 2000. Liquefaction resistance of soils from shear-wave velocity, *J.*
502 *Geotech. Geoenviron. Eng.* **126(11)**, 1015-1025.
- 503 Boulanger, R. W. and Idriss, I. M., 2012. Probabilistic standard penetration test-based liquefaction-
504 triggering procedure, *J. Geotech. Geoenviron. Eng.* **138**, 1185-1195.
- 505 Boulanger, R. W. and Idriss, I. M., 2016. CPT-based liquefaction triggering procedure, *J. Geotech.*
506 *Geoenviron. Eng.* **142(2)**, 04015065.
- 507 Boulanger, R. W. and DeJong, J. T., 2018. Inverse filtering procedure to correct cone penetration data
508 for thin-layer and transition effects, Proc. 4th International Symposium on Cone Penetration Testing
509 (CPT'18), 21-22 June, Delft, The Netherlands.
- 510 Bozorgnia, Y., Abrahamson, N. A., Al Atik, L., Ancheta, T. D., Atkinson, G. M., Baker, J. W., Baltay,
511 A., Boore, D. M., Campbell, K. W., Chiou, B. S.-J., Darragh, R., Day, S., Donahue, J., Graves, R.
512 W., Gregor, N., Hanks, T., Idriss, I. M., Kamai, R., Kishida, T., Kottke, A., Mahin, S. A., Rezaeian,
513 S., Rowshandel, B., Seyhan, E., Shahi, S., Shantz, T., Silva, W., Spudich, P., Stewart, J. P., Watson-

514 Lamprey, J., Wooddell, K., and Youngs, R. R., 2014. NGA-West2 research project, *Earthquake*
515 *Spectra* **30**, 973–987.

516 Brandenburg, S. J. and Zimmaro, P., 2019a. Next Generation Liquefaction (NGL) Partner Dataset -
517 Sample Queries, DesignSafe-CI, Dataset, doi:10.17603/ds2-xvp9-ag60.

518 Brandenburg, S. J. and Zimmaro, P., 2019b. Next Generation Liquefaction (NGL) Partner Dataset -
519 Cone Penetration Test (CPT) Viewer, DesignSafe-CI, Dataset, doi:10.17603/ds2-99kp-rw11.

520 Brandenburg, S. J. and Zimmaro, P., 2019c. Next Generation Liquefaction (NGL) Partner Dataset -
521 Surface Wave Viewer, DesignSafe-CI, Dataset, doi:10.17603/ds2-cmn0-h864.

522 Brandenburg, S. J., Goulet, C. A. Wang, P., Nweke, C., Davis, C., Buckreis, T., Issa, O., Liu, Z., Kim,
523 Y., Zareian, F., Hudnut, K., Fayaz, J., Hudson, M., Hudson, K., Lyda, A., Ahdi, S., Stewart, J. P.,
524 Yeung, J. S., Donnellan, A., Lyzenga, G., Winters, M. A., Lucey, J. T. D., Gallien, T. W., Meng,
525 X., Kim, Y., Delisle, M.-P. C.; Yi, Z., 2019. Ridgecrest, CA earthquake sequence, July 4 and 5,
526 2019. DesignSafe-CI. doi: 10.17603/ds2-4thk-d514.

527 Brandenburg, S. J., Kwak, D. Y., Zimmaro, P., Bozorgnia, Y., Kramer, S. L., and Stewart, J. P., 2018.
528 Next-Generation Liquefaction (NGL) Case History Database Structure. Fifth decennial GEESD
529 Conference, Austin, TX (USA), June 10-13. *Geotechnical Special Publication* **290**, 426-433.

530 Brandenburg, S. J. Zimmaro, P., Lee, A., Fisher, H., Stewart, J. P. 2019. Next Generation Liquefaction
531 (NGL) Partner Dataset, DesignSafe-CI, Dataset, doi:10.17603/ds2-2xzy-1y96.

532 Çetin, K. O., Seed, R. B., Der Kiureghian, A., Tokimatsu, K., Harder, L. F., Kayen, R. E., Moss, R. E.
533 S., 2004. SPT-based probabilistic and deterministic assessment of seismic soil liquefaction
534 potential, *J. Geotech. Geoenviron. Eng.* **130(12)**, 1314-1340.

535 Çetin, K. O., Seed, R. B., Kayen, R. E., Moss, R. E. S., Bilge, H. T., Ilgac, M., and Chowdhury, K.
536 2018. SPT-based probabilistic and deterministic assessment of seismic soil liquefaction triggering
537 hazard, *Soil Dyn. Earthquake Eng.* **115**, 698-709.

538 Foti, S., Hollender, F., Garofalo, F., Albarello, D., Asten, M., Bard, P.-Y., Comina, C., Cornou, C.,
539 Cox, B., Di Giulio, G., Forbriger, T., Hayashi, K., Lunedei, E., Martin, A., Mercerat, D.,
540 Ohrnberger, M., Poggi, V., Renalier, F., Sicilia, D., Socco, V., 2017. Guidelines for the good
541 practice of surface wave analysis: a product of the InterPACIFIC project, *Bull Earthq Eng* **16**,
542 2367–2420.

543 Franke, K. W., Rollins, K. M., Ledezma, C., Hedengren, J. D., Wolfe D., Ruggles S., Bender C., and
544 Reimschiessel B., 2017. Reconnaissance of two liquefaction sites using small unmanned aerial
545 vehicles and structure from motion computer vision following the April 1, 2014 Chile earthquake,
546 *J. Geotech. Geoenviron. Eng.* **143(5)**, 04016125.

547

548 Goulet, C. A., Bozorgnia, Y., Abrahamson, N. A., Kuehn, N., Al Atik, L., Youngs, R. R., and Graves,
549 R. W. 2018. Central and Eastern North America Ground-Motion Characterization - NGA-East Final
550 Report, PEER Report 2018/08, Pacific Earthquake Engineering Research Center, Berkeley, CA.

551 Greenfield, M. W. 2017. Effects of long-duration ground motions on liquefaction hazards. Ph.D.
552 Dissertation, University of Washington.

553 Imakiire, T. and Koarai, M. 2012. Wide-area land subsidence caused by the 2011 off the Pacific Coast
554 of Tohoku earthquake, *Soils Found.* **52**, 842–855.

555 Kayen, R. E., Moss, R. E. S., Thompson, E. M., Seed, R. B., Çetin, K. O., Der Kiureghian, A., Tanaka,
556 Y., and Tokimatsu, K. 2013. Shear-wave velocity–based probabilistic and deterministic assessment
557 of seismic soil liquefaction potential, *J. Geotech. Geoenviron. Eng.* **139**, 407-419.

558 Kishida, T., Bozorgnia, Y., Abrahamson, N. A., Ahdi, S. K., Ancheta, T. D., Boore, D. M., Campbell,
559 K. W., Darragh, R. B., Magistrale, H., and Stewart J. P. 2017. Development of NGA-Subduction
560 database, *Proc. 16th World Conf. on Earthquake Eng.*, Santiago, Chile (Paper No. 3452).

561 Konagai, K., Kiyota, T., Suyama, S., Asakura, T., Shibuya, K., and Eto, C. 2013. Maps of soil
562 subsidence for Tokyo bay shore areas liquefied in the March 11th, 2011 off the Pacific Coast of
563 Tohoku earthquake, *Soil Dyn. Earthquake Eng.* **53**, 240–253.

564 Kramer, S. L. and Mitchell, R. A. 2006. Ground Motion Intensity Measures for Liquefaction Hazard
565 Evaluation, *Earthquake Spectra* **22**, 413-438.

566 Kramer, S. L., Sideras, S. S., and Greenfield, M. W. 2016. The timing of liquefaction and its utility in
567 liquefaction hazard evaluation, *Soil Dyn. Earthquake Eng.* **91**, 133–146.

568 Kwak, D. Y., Stewart, J. P., Brandenburg, S. J., and Mikami, A. 2016. Characterization of seismic levee
569 fragility using field performance data, *Earthquake Spectra* **32**, 193–215.

570 Lee, A., Fisher, H., Zimmaro, P., Brandenburg, S.J. 2019. Next Generation Liquefaction (NGL) Partner
571 Dataset - Boring Log Viewer, DesignSafe-CI, Dataset, doi:10.17603/ds2-sj7t-av93.

572 Lewis M. R., Arango, I., Kimball, J. K., and Ross, T. E. 1999. Liquefaction resistance of old sand
573 deposits. Proc., 11th Panamerican Conference on Soil Mechanics and Geotechnical Engineering,
574 Foz do Iguassu, Brasil, 821-829.

575 Maurer, B. W., Green R. A., and Taylor, O.-D. S. 2014. Moving towards an improved index for
576 assessing liquefaction hazard: Lessons from historical data, *Soils and Foundations* **55**, 778-787.

577 Maurer, B. W., Green R. A., Cubrinovski, M., and Bradley, B. 2014. Evaluation of the Liquefaction
578 Potential Index for Assessing Liquefaction Hazard in Christchurch, New Zealand, *Journal of*
579 *Geotechnical and Geoenvironmental Engineering* **140**, 04014032.

580 Moss, R. E. S., Seed, R. B. Kayen, R. E., Stewart, J. P., Der Kiureghian, A., Çetin, K. O. 2006. CPT-
581 based probabilistic and deterministic assessment of in situ seismic soil liquefaction potential, *J.*
582 *Geotech. Geoenviron. Eng.* **132**, 1032-1051.

583 National Academies of Sciences, Engineering, and Medicine. 2016. *State of the Art and Practice in the*
584 *Assessment of Earthquake-Induced Soil Liquefaction and Its Consequences*. Washington, DC: The
585 National Academies Press. doi: 10.17226/23474.

586 Obermeier, S. F., Jacobson, R. B., Smoot, J. P., Weems, R. E., Gohn, G. S., Monroe, J. E., and Powars,
587 D. S. 1990. Earthquake-induced liquefaction features in the coastal setting of South Carolina and
588 in the fluvial setting of the New Madrid seismic zone, U.S. Geological Survey Professional Paper
589 1504, U.S. Government Printing Office, Washington, D.C.

590 Olsen, M. J., Cheung, K. F., Yamazaki, Y., Butcher, S., Garlock, M., Yim, S., McGarity, S., Robertson,
591 I., Burgos, L., and Young, Y. L., 2012. Damage assessment of the 2010 Chile earthquake and
592 tsunami using terrestrial laser scanning, *Earthquake Spectra* **28(S1)**, S179–S197.

593 Pérez, F. and Granger, B.E., 2007. IPython: A System for Interactive Scientific Computing, *Computing*
594 *in Science and Engineering* **9(3)**, 21-29, doi:10.1109/MCSE.2007.53. URL: <https://ipython.org>

595 Rathje, E. M., Dawson, C., Padgett, J. E., Pinelli, J.-P., Stanzione, D., Adair, A., Arduino, P.,
596 Brandenburg, S. J., Cockeril, T., Esteva, M., Haan, F. L. Jr., Hanlon, M., Kareem, A., Lowes, L.,
597 Mock, S., and Mosqueda, G. 2017. DesignSafe: A new cyberinfrastructure for natural hazards
598 engineering, *Natural Hazards Review* **18(3)**.

599 Rathje, E. M., Secara S. S., Martin, J. G., van Ballegooy, S., and Russell, J., 2017. Liquefaction-induced
600 horizontal displacements from the Canterbury earthquake sequence in New Zealand measured from
601 remote sensing techniques, *Earthquake Spectra* **33**, 1475-1494.

602 Robertson, P. K. and Wride, C. E. 1998. Evaluating cyclic liquefaction potential using the cone
603 penetration test, *Canadian Geotechnical Journal*, **35(3)**, 442-459.

604 Seed, H. B., Idriss, I. M., and Arango, I. 1983. Evaluation of liquefaction potential using field
605 performance data, *J. Geotech. Engrg.* **109(3)**, 458-482.

606 Smith, G.I., 2009. Late Cenozoic geology and lacustrine history of Searles Valley, Inyo and San
607 Bernardino Counties, California: U.S. Geological Survey Professional Paper 1727, 115 p., 4 plates.

608 Stafford, P. J. 2012. Evaluation of structural performance in the immediate aftermath of an earthquake:
609 A case study of the 2011 Christchurch earthquake, *Int. J. Forensic Engrg.* **1**, 58-77.

610 Stewart, J. P., Kramer, S. L., Kwak, D. Y., Greenfield, M. W., Kayen, R. E., Tokimatsu, K., Bray, J.
611 D., Beyzaei, C. Z., Cubrinovski, M., Sekiguchi, T., Nakai, S., Bozorgnia, Y. 2016. PEER-NGL
612 project: Open source global database and model development for the next-generation of
613 liquefaction assessment procedures, *Soil Dyn. Earthquake Eng.* **91**, 317–328.

614 Stewart, J.P. (ed.), Brandenberg, S.J., Wang, Pengfei, Nweke, C.C., Hudson, K., Mazzoni, S.,
615 Bozorgnia, Y., Hudnut, K.W., Davis, C.A., Ahdi, S.K., Zareian, F., Fayaz, J., Koehler, R.D.,
616 Chupik, C., Pierce, I., Williams, A., Akciz, S., Hudson, M.B., Kishida, T., Brooks, B.A., Gold,
617 R.D., Ponti, D.J., Scharer, K.M., McPhillips, D.F., Ericksen, T., Hernandez, J., Patton, J., Olson,
618 B., Dawson, T., Treiman, J., Duross, C.B., Blake, K., Buchhuber, J., Madugo, C., Sun, J.,
619 Donnellan, A., Lyzenga, G., and Conway, E., 2019. Preliminary report on engineering and
620 geological effects of the July 2019 Ridgecrest Earthquake sequence: Geotechnical Extreme Events
621 Reconnaissance Association Report GEER-064, doi: 10.18118/G6H66K.

622 van Ballegooy, S., Malan, P., Lacrosse, V., Jacka, M. E., Cubrinovski, M., Bray, J. D., O'Rourke, T.
623 D., Crawford, S. A., and Cowan H., 2014. Assessment of Liquefaction-Induced Land Damage for
624 Residential Christchurch, *Earthquake Spectra* **30**, 31-55.

625 Winters, M. A. Delisle, M.-P. C. Lucey, J.T. D. Kim, Y. Liu, Z. Hudson, K. Brandenberg, S. and
626 Gallien, T. W. 2019. UCLA UAV Imaging in Ridgecrest, CA Earthquake Sequence, July 4 and 5,
627 2019. DesignSafe-CI, Dataset, doi: 10.17603/ds2-wfgc-a575.

628 Youd, T. L. and Hoose, S. N. 1978. Historic ground failures in Northern California triggered by
629 earthquakes., U.S. Geological Survey, Professional Paper 993. Available at:
630 <http://pubs.usgs.gov/pp/1978/pp0993/>.

631 Youd, T. L. and Perkins D. M. 1978. Mapping liquefaction-induced ground failure potential. *Journal*
632 *of the Geotechnical Engineering Division* 104(4), 433–446.

633 Zhu, J., Baise, L. G., Thompson, E. M. 2017. An updated geospatial liquefaction model for global
634 application, *Bulletin of the Seismological Society of America* **107**, 1365-1385.

635 Zhu, J., Daley, D., Baise, L. G., Thompson, E. M., Wald, D. J., and Knudsen, K. L. 2015. A geospatial
636 liquefaction model for rapid response and loss estimation, *Earthquake Spectra* **31**, 1813-1837.

637 Zimmaro, P. and Brandenberg, S. J., 2019. Next Generation Liquefaction (NGL) Partner Dataset -
638 Invasive Geophysical Test Viewer, DesignSafe-CI, Dataset, doi:10.17603/ds2-tq39-kp49.

639 Zimmaro, P., Brandenberg, S. J., Bozorgnia, Y., Stewart, J. P., Kwak, D. Y., Çetin, K. O., Can, G.,
640 Ilgac, M., Franke, K. W., Moss, R. E. S., Kramer, S. L., Stamatakos, J., Juckett, M., and Weaver,

641 T. 2019b. Quality Control for Next-Generation Liquefaction Case Histories. *VII International*
642 *Conference on Earthquake Geotechnical Engineering*, Rome, Italy, 17-20 June, 2019, . In
643 *Earthquake Geotechnical Engineering for Protection and Development of Environment and*
644 *Constructions – Silvestri & Moraci (Eds)*, 5905-5912.

645 Zimmaro, P., Brandenberg, S. J., Stewart, J. P., Kwak, D. Y., Franke, K. W., Moss, R. E. S., Çetin, K.
646 O., Can, G., Ilgac, M., Stamatakos, J., Juckett, M., Mukherjee, J., Murphy, Z., Ybarra, S., Weaver,
647 T., Bozorgnia, Y., and Kramer, S. L. 2019a. Next-Generation Liquefaction Database. Next-
648 Generation Liquefaction Consortium. doi: 10.21222/C2J040.